Cross-Bridge Kelvin Resistor (CBKR) Structures for Measurement of Low Contact Resistances

N. Stavitski, *Student Member, IEEE*, J.H. Klootwijk, *Member, IEEE*,
H.W. van Zeijl, B.K. Boksteen, A.Y. Kovalgin, R.A.M. Wolters

***Abstract*—A convenient test structure for measurement of the specific contact resistance (ρ_c) of metal-semiconductor junctions is the CBKR structure. During last few decades the parasitic factors which may strongly affect the measurements accuracy for $\rho_c < 10^{-6}\ \Omega \cdot \mathrm{cm}^2$ have been sufficiently discussed and the minimum of the ρ_c to be measured using CBKR structures was estimated. We fabricated a set of CBKR structures with different geometries to confirm this limit experimentally. These structures were manufactured for metal-to-metal contacts. It was found that the extracted CBKR values were determined by dimensions of the two-metal stack in the contact area and sheet resistances of the metals used.**

***Index Terms*—Contact resistance, cross-bridge Kelvin resistor (CBKR), sheet resistance, test structures, metal, silicon**

I. INTRODUCTION

CBKR structures are the mostly used test structures to characterize metal-semiconductor contacts in the planar devices of VLSI technology [1, 2]. On the other hand, CBKR is very sensitive to lateral current crowding around the contact when the contact window is smaller than the underlying layer. This lateral current flow induces an additional voltage drop (i.e. additional resistance R_{geom}) at the contact periphery. For high quality contacts with low specific contact resistances and for materials with high sheet resistances, such as silicide-to-silicon contacts, R_{geom} becomes extremely important [3, 4]. Several simulations and correction methods were introduced in order to account for the current crowding effect [5-8]. However in the low resistance range, the extracted specific contact resistance values, obtained using CBKR structures, were still orders of magnitude different from the results obtained using other methods [2]. A possible explanation of this phenomenon is the lack of accuracy during the data extraction using CBKR structures, when ρ_c is in the range of $10^{-8}\ \Omega{\cdot}\mathrm{cm}^2$ and below [9]. In this case, the lateral current flow around the contacts accounts for an even higher additional R_{geom} [3, 4]. This effect becomes worse for a lower ρ_c and a higher sheet resistance (R_{sh}) of the underlying layer. The simulations show that, for $\rho_c < 10^{-7}$ $\Omega{\cdot}\mathrm{cm}^2$, the extracted ρ_c can differ by one or two orders of magnitude from the actual value [8]. Unfortunately, the trend in the technology of today's high-density integrated circuits is towards a lower ρ_c and a higher R_{sh} (due to shallower junctions). This will further complicate the interpretation of CBKR measurements.

Our research is therefore concerned with experimental finding of the validity range for CBKR measurements in terms of the *minimal* resistance to be measured with this technique. For that purpose, CBKR structures of different geometries were designed and manufactured. These structures were evaluated for metal-to-metal contacts to provide the case of very low contact resistances.

II. MEASUREMENT TECHNIQUE AND TEST STRUCTURES DESCRIPTION

The standard four-terminal CBKR is used to determine ρ_c of metal-to-metal contacts (Fig. 1). The measurement

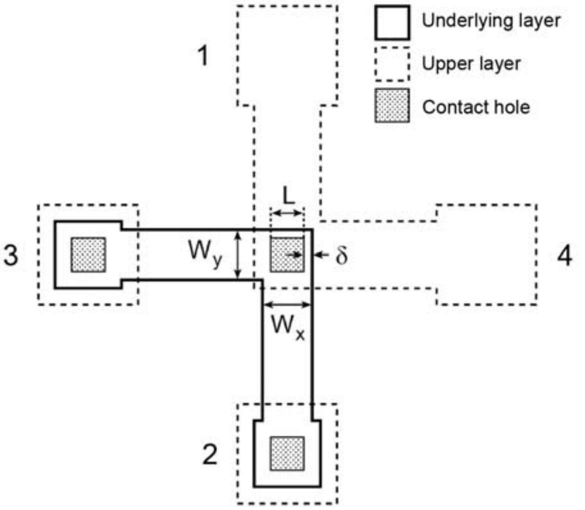

Fig. 1. Schematic view of four-terminal CBKR structure with contact geometry parameters definition. The contact geometry parameters (δ and L) for both layers are identical in this work.

This project is supported by NXP Research.

N. Stavitski, A. Y. Kovalgin, B.K. Boksteen and J. Schmitz are with MESA+ Institute for Nanotechnology, Chair of Semiconductor Components, University of Twente, Enschede, The Netherlands (e-mail: n.stavitski@utwente.nl).

J.H. Klootwijk is with Philips Research, prof. Holstlaan 4, 5656 AA Eindhoven, The Netherlands

H.W. van Zeijl is with DIMES, Delft University of Technology, Feldmannweg 17, 2628 CT Delft, The Netherlands

R. A. M. Wolters is with MESA+ Institute for Nanotechnology, Chair of Semiconductor Components, University of Twente, Enschede, The Netherlands and NXP Research Eindhoven, Prof. Holstlaan 4, 5656 AA Eindhoven, The Netherlands.

principle consists of forcing the current (I) between contacts 1 and 2 and measuring the voltage drops (V_{34}) between contacts 3 and 4: $V_{34} = V_3 - V_4$. The contact resistance R_k can be then found as

$$R_\mathrm{k} = \frac{V_{34}}{I}. \qquad (1)$$

In the 1D-Model approach [6], the specific contact resistance can be calculated directly from the contact area A and assuming $R_c = R_k$:

$$\rho_\mathrm{c} = R_\mathrm{c} A. \qquad (2)$$

The 1D-Model does not account for the current flowing in the overlap region (δ) between the contact edge and the underlying layer sidewall. In the ideal case with $\delta = 0$ (Fig. 2a), the voltage drop is $V_{34} = IR_c$. For $\delta > 0$ (Fig. 2b), the lateral current flow gives an additional voltage drop that is included in V_{34}, leading to higher voltage.

In that case the so-called 2D-Model should be applied [6]. In this work an analytical model by Schreyer and Saraswat was used for this correction. The actually measured resistance (R_k) is then a sum of the resistance due to the voltage drop across the actual contact (R_c) and the resistance due to the current flow around the contact in the overlap region (R_{geom}) (3). The ρ_c can further be extracted from (4), where R_{sh} is the sheet resistance of the underlying layer. The contact geometry parameters are presented in Fig. 1.

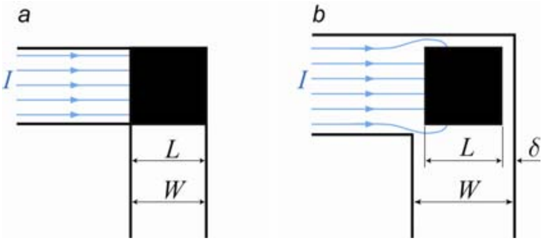

Fig. 2. Schematic of a current flow in a four-terminal CBKR test structure. (a) Ideal case with current flow in the contact only ($\delta = 0$). (b) Real case with current flowing through the contact and the overlap region ($\delta > 0$).

$$R_\mathrm{k} = R_\mathrm{c} + R_\mathrm{geom} \qquad (3)$$

$$R_\mathrm{k} = \frac{\rho_\mathrm{c}}{A} + \frac{4R_\mathrm{sh}\delta^2}{3W_\mathrm{x}W_\mathrm{y}}\left[1 + \frac{\delta}{2(W_\mathrm{x} - \delta)}\right] \qquad (4)$$

In order to verify the validity of the results obtained, the CBKR structures were designed to cover a wide range of contact sizes (L_x, L_y) and overlap sizes (δ) between metal layer (with the width of W_x, W_y) and the contact hole. The details are summarized in Table I. An example of a CBKR structure is presented in Fig. 3.

TABLE I
SUMMARY ON THE REALIZED CBKR TEST STRUCTURES

Geometry	Contact size ($L_x = L_y$, µm)	Overlap size (δ, µm)
Square	1	0.2, 0.5, 1, 2, 5
Square	2	0.2, 0.5, 1, 2, 5
Square	4.43	0.2, 0.5, 1, 2, 5
Square	8.86	0.2, 0.5, 1, 2, 5
Square	17.72	0.2, 0.5, 1, 2, 5

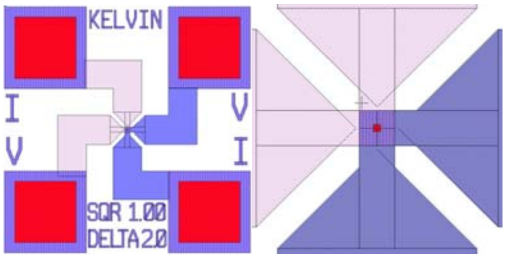

Fig. 3. An example of the newly-designed square CBKR structure. The complete structure (on the left-) and a blow up of the actual contact (on the right-hand size).

III. TEST STRUCTURES FABRICATION

The (100) p-type Si wafers with 1 µm-thick thermal oxide were used as a starting material for the structure fabrication. First, a 0.675 µm-thick Al layer was sputtered and patterned using I-line lithography and plasma etching. Then, a 0.8 µm-thick layer of SiO_2 was deposited by PECVD and the contact holes were opened. Prior to the second Al deposition, the contacts were in-situ RF-precleaned. The second Al layer of 1.4 µm was sputtered and patterned as the front metallization layer, including the bond pads. Finally, the structure received a 20min alloying at 400 °C in N_2/H_2 mixture.

IV. RESULTS AND DISCUSSION

A large variety of test structures with different contact and

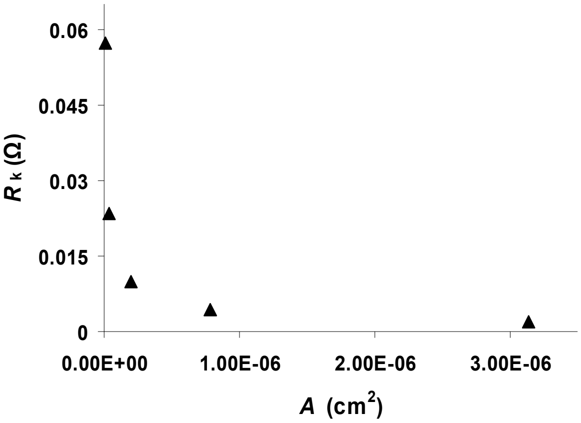

Fig. 4. Measured contact resistance vs. contact size for given overlap size of 2 µm.

overlap sizes was measured using the standard 4-point Kelvin mode. The measured Kelvin resistance R_k is plotted as a function of contact size ($A = L_x L_y$) and the overlap size (δ), as shown in Fig. 4 and Fig. 5, respectively. R_k increases with increasing δ and it decreases with increasing contact size. This is in agreement with the theory (4). The specific contact resistance was extracted using both 1D- and 2D-approximations and plotted as a function of the contact and overlap size (Fig. 6 and Fig. 7, respectively). The obtained results supported the earlier discussed importance of applying the advanced 2D-Model instead of the simplest 1D approximation, in particular for low contact resistance values. The results, obtained for different contact sizes, revealed similar behavior. The extracted ρ_c values (A = 4 µm) were 5.4 • 10^{-10} $\Omega \cdot cm^2$ (Fig. 7). The sheet resistances of both the back and front metal layers were measured using the Van-der-Pauw test structures, fabricated on the same wafers. The obtained values were 0.0054 and 0.0027 Ω/□ for the back and front metals, respectively, in agreement with the corresponding thicknesses. The estimated resistance, determined by dimensions of the two-metal stack in the contact area and their sheet resistances, agreed with the measured R_k values, providing the minimum value to be accurately extracted from the CBKR structures.

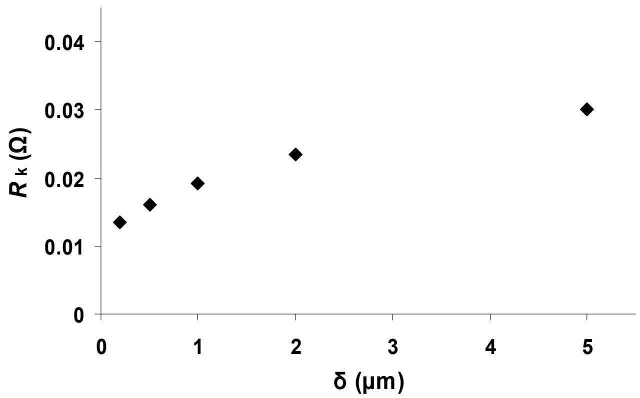

Fig. 5. Measured Kelvin resistance vs. overlap size for a contact size of 4 µm.

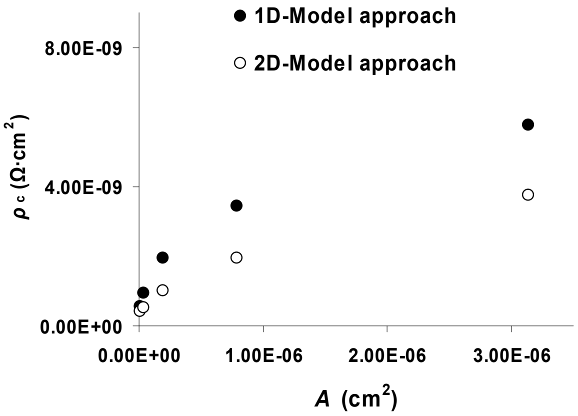

Fig. 6. Extracted specific contact resistance vs. contact size for an overlap size of *2* µm.

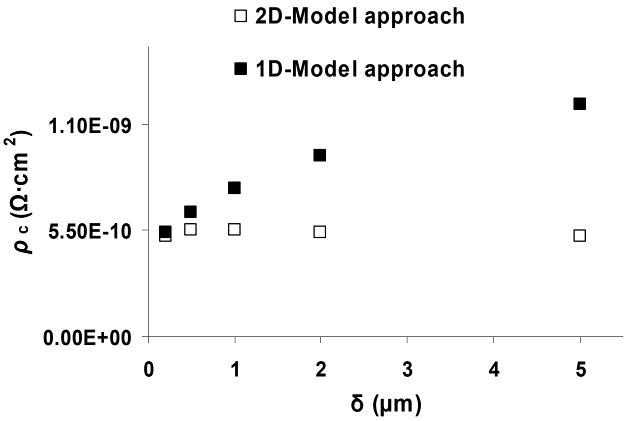

Fig. 7. Extracted specific contact resistance vs. overlap size for a contact size of 4 µm.

CONCLUSIONS

A new design of metal-to-metal CBKR structures has been realized. The structures included a large variety of contact geometries and feature sizes for contact holes and overlap regions. The obtained results were in agreement with the analytical model proposed by Schreyer and Saraswat, demonstrating the necessity to account for 2D current flow effects while measuring low contact resistance values. The specific contact resistance, extracted for the metal-to-metal contacts, corresponded to the pure resistance of the two-metal stack in the area of contact, obtained from both the stack dimensions and metal sheet resistances. This determined the minimum value to be accurately extracted from the CBKR structures.

ACKNOWLEDGEMENTS

The authors would like to thank the DIMES Clean room staff of Delft University of Technology for processing the wafers.

REFERENCES

[1] S. Wolf and R. N. Tauber, *Silicon Processing for the VLSI Era*, ed., vol. 2. Sunset Beach: Lattice Press, 1986.

[2] D. K. Schroder, *Semiconductor Material and Device Characterization*, 3rd ed. New York: Wiley-Interscience/IEEE, 2006.

[3] A. Scorzoni, M. Finetti, K. Grahn, I. Suni, and P. Cappelletti, "Current Crowding and Misalignment Effects as Sources of Error in Contact Resistivity Measurements .1. Computer-Simulation of Conventional Cer and Ckr Structures," *IEEE Trans. Electron Devices,* vol. 34, pp. 525-531, Mar. 1987.

[4] W. M. Loh, K. Saraswat, and R. W. Dutton, "Analysis and Scaling of Kelvin Resistors for Extraction of Specific Contact Resistivity," *IEEE Electron Device Lett.,* vol. 6, pp. 105-108, 1985.

[5] W. M. Loh, S. E. Swirhun, E. Crabbe, K. Saraswat, and R. M. Swanson, "An Accurate Method to Extract Specific Contact Resistivity Using Cross-Bridge Kelvin Resistors," *IEEE Electron Device Lett.,* vol. 6, pp. 441-443, 1985.

[6] T. A. Schreyer and K. C. Saraswat, "A Two-Dimensional Analytical Model of the Cross-Bridge Kelvin Resistor," *IEEE Electron Device Lett.,* vol. 7, pp. 661-663, Dec. 1986.

[7] J. Santander, M. Lozano, A. Collado, M. Ullan, and E. Cabruja, "Accurate contact resistivity extraction on Kelvin structures with upper and lower resistive layers," *IEEE Trans. Electron Devices,* vol. 47, pp. 1431-1439, Jul. 2000.

[8] A. S. Holland, G. K. Reeves, and P. W. Leech, "Universal error corrections for finite semiconductor resistivity in Cross-Kelvin resistor test structures," *IEEE Trans. Electron Devices,* vol. 51, pp. 914-919, Jun. 2004.

[9] R. L. Gillenwater, M. J. Hafich, and G. Y. Robinson, "Extraction of the Minimum Specific Contact Resistivity Using Kelvin Resistors," *IEEE Electron Device Lett.,* vol. 7, pp. 674-676, Dec. 1986.